Spontaneous Action Potentials due to Channel Fluctuations

Carson C. Chow* and John A. White#
*NeuroMuscular Research Center and #Department of Biomedical Engineering, Boston University, Boston, Massachusetts 02215 USA

ABSTRACT A theoretical and numerical analysis of the Hodgkin-Huxley equations with the inclusion of stochastic channel dynamics is presented. It is shown that the system can be approximated by a one-dimensional bistable Langevin equation. Spontaneous action potentials can arise from the channel fluctuations and are analogous to escape by a particle over a potential barrier. The mean firing rate can be calculated using Kramers' classic result for barrier escape. The probability density function of the interspike intervals can also be estimated. The analytical results compare favorably with numerical simulations of the complete stochastic system.

INTRODUCTION

Neuronal action potentials, generated by the concerted actions of populations of ion channels, can typically be modeled with great success using some variant of the classic phenomenological model of Hodgkin and Huxley (1952). However, individual ion channels are probabilistic devices (Hille, 1992), and recent work indicates that fluctuations in the states of these devices may be physiologically important in small neuronal structures like nodes of Ranvier (see, e.g., Skaugen and Walløe, 1979; Sigworth, 1980; Strassberg and De Felice, 1993; Rubinstein, 1995).

Here, we study the generation of noise-induced action potentials due to ion channel fluctuations analytically and numerically. Previously, it had been demonstrated that the Hodgkin-Huxley model with discrete Markovian ion kinetics instead of the usual continuous rate equations can lead to spontaneous generation of action potentials (Lecar and Nossal, 1971b; Skaugen and Walløe, 1979; Strassberg and De Felice, 1993, De Felice and Goolsby, 1996). Numerical simulations show that as the membrane area (number of ion channels) is reduced, spontaneous firing can occur for a subthreshold injected current. The firing arises entirely from stochastic fluctuations of the ion channels. The spontaneous firing rate decreases as the number of ion channels increases. There is a critical channel number where the spontaneous action potentials cease to exist. It is of interest to understand these effects theoretically.

A comprehensive theoretical study of spontaneous firing due to noise was done by Lecar and Nossal (1971a, 1971b) by linearizing around the threshold. More recently, a detailed stochastic analysis of the Hodgkin-Huxley system with random Markovian ion kinetics was performed by Fox and Lu (1994) where it was shown how the membrane dynamics converges to a deterministic limit as the number of ion channels increases. In this study, we retain the essential nonlinearity of the membrane to obtain a closed-form expression for the firing rate of spontaneous action potentials for subthreshold input. We find that it has a negative exponential dependence with the number of ion channels. The characteristic channel number is given by the parameters of the Hodgkin-Huxley equation. We also show that the distribution of the spontaneous interspike intervals approximately obeys a displaced negative exponential distribution with a characteristic time scale given by the mean firing rate. The theory can be generalized to other membrane equations to give a reasonable estimate of when discrete ion effects are important. To corroborate our analytical results we have conducted numerical simulations. Using an efficient algorithm, we performed high-precision simulations of the stochastic Hodgkin-Huxley system, including probabilistic descriptions of Na^+ channel activation and inactivation, as well as K^+ channel activation. We find that simulated results match with the analytical results.

MEMBRANE DYNAMICS

The membrane equation of the Hodgkin-Huxley model describing the squid giant axon is given by (Hodgkin and Huxley, 1952)

$$C\frac{dV}{dt} = -[g_L(V - V_L) + g_K(V - V_K) + g_{Na}(V - V_{Na}) - I], \quad (1)$$

where V is the membrane potential, V_L is the resting leakage potential for a leakage conductance g_L, V_K and V_{Na} are the potassium and sodium reversal or Nernst potentials, C is the capacitance and I is an injected current. The classic values of these parameters used by Hodgkin and Huxley (1952) for a temperature of 6.3°C is shown in Table 1 (note that the modern convention for membrane potential is used). The voltage-dependent membrane conductances for the potassium and sodium channels are given by

$$g_K = \bar{g}_K\frac{Q_K}{N_K}, \quad g_{Na} = \bar{g}_{Na}\frac{Q_{Na}}{N_{Na}}, \quad (2)$$

Received for publication 29 April 1996 and in final form 10 September 1996.

Address reprint requests to Dr. John A. White, Department of Biomedical Engineering, Boston University, 44 Cummington St., Boston, MA 02215. Tel.: 617-353-5903; Fax: 617-353-6766; E-mail: jwhite@bu.edu.

Current address for Carson Chow: Department of Mathematics, Boston University, 111 Cummington St., Boston MA 02215, E-mail: ccc@bu.edu.

0006-3495/96/12/3013/09 $2.00

TABLE 1 Parameters used in the theory and simulations

C	Membrane capacitance	1 μF/cm^2
V_L	Leakage reversal potential	−54.4 mV
g_L	Leakage conductance	0.3 mS/cm^2
V_K	Potassium reversal potential	−77 mV
$\bar{g}_K$	Maximal potassium conductance	36 mS/cm^2
ρ_K	Potassium ion channel density	18 channels/μm^2
N_K	Number of potassium channels	
N_{n_k}	Number of potassium channels in state n_k	
V_{Na}	Sodium reversal potential	50 mV
$\bar{g}_{Na}$	Maximal sodium conductance	120 mS/cm^2
ρ_{Na}	Sodium ion channel density	60 channels/μm^2
N_{Na}	Number of sodium channels	
$N_{m_ih_j}$	Number of sodium channels in state m_ih_j	

where Q_K and Q_{Na} are the number of "open" potassium and sodium channels; N_K and N_{Na} are the total number of potassium channels, given by the equations $N_K = \rho_K \times$ Area, and $N_{Na} = \rho_{Na} \times$ Area, where ρ_K and ρ_{Na} are the K^+ and Na^+ channel densities, respectively; and $\bar{g}_K$ and $\bar{g}_{Na}$ give the maximum conductance densities when all the channels are open.

Hodgkin and Huxley (1952) found that the electrical properties of the squid giant axon were well modeled by considering conductance to be governed by the states of a finite number of independent binary "gates." In the modern view, one could consider these gates to be relevant at the single channel level. A given channel would only conduct when all of its composite gates were in the open position. In this scheme, the potassium channel is composed of four identical gates, while the sodium channel is composed of three identical "activating" gates and one "inactivating" gate. The opening and closing of these gates are inherently probabilistic. In classical analyses of voltage-clamp data, only the mean values of the fraction of open channels are considered. This is a valid approximation for large numbers of channels in a large patch of membrane. However, for a small patch, statistical fluctuations will play a role.

Assuming a simple Markov process for four identical gates with an opening rate α_n and a closing rate of β_n, the kinetic scheme for the potassium channel is given by (Skaugen and Walløe, 1979; Hille, 1992; Strassberg and De Felice, 1993)

$$n_0 \underset{\beta_n}{\overset{4\alpha_n}{\rightleftharpoons}} n_1 \underset{2\beta_n}{\overset{3\alpha_n}{\rightleftharpoons}} n_2 \underset{3\beta_n}{\overset{2\alpha_n}{\rightleftharpoons}} n_3 \underset{4\beta_n}{\overset{\alpha_n}{\rightleftharpoons}} n_4, \tag{3}$$

where n_4 corresponds to the open state where all four gates are open. The Markov kinetic scheme for the Na^+ channel is given by

$$\begin{array}{ccccc} m_0h_1 & \underset{\beta_m}{\overset{3\alpha_m}{\rightleftharpoons}} & m_1h_1 & \underset{2\beta_m}{\overset{2\alpha_m}{\rightleftharpoons}} & m_2h_1 & \underset{3\beta_m}{\overset{\alpha_m}{\rightleftharpoons}} & m_3h_1 \\ \alpha_h \Updownarrow \beta_h & & \alpha_h \Updownarrow \beta_h & & \alpha_h \Updownarrow \beta_h & & \alpha_h \Updownarrow \beta_h \\ m_0h_0 & \underset{\beta_m}{\overset{3\alpha_m}{\rightleftharpoons}} & m_1h_0 & \underset{2\beta_m}{\overset{2\alpha_m}{\rightleftharpoons}} & m_2h_0 & \underset{3\beta_m}{\overset{\alpha_m}{\rightleftharpoons}} & m_3h_0, \end{array} \tag{4}$$

where m_3h_1 corresponds to the open state where the three activating m gates and the inactivating h gate are open.

For the classic parameters of Table 1 the voltage-dependent rate constants have the form

$$\alpha_n = \frac{0.01(V+55)}{1-e^{-(V+55)/10}}, \quad \beta_n = 0.125e^{-(V+65)/80}, \tag{5}$$

$$\alpha_m = \frac{0.1(V+40)}{1-e^{-(V+40)/10}}, \quad \beta_m = 4e^{-(V+65)/18}, \tag{6}$$

$$\alpha_h = 0.07e^{-(V+65)/20}, \quad \beta_h = \frac{1}{1+e^{-(V+35)/10}}, \tag{7}$$

where V has units of mV and the rates have units of ms^{-1}.

In the continuous limit for the classic Hodgkin-Huxley equations, the conductances satisfy

$$g_K = \bar{g}_K n^4 \quad g_{Na} = \bar{g}_{Na} m^3 h, \tag{8}$$

where

$$\frac{dn}{dt} = \alpha_n(1-n) - \beta_n n, \tag{9}$$

$$\frac{dm}{dt} = \alpha_m(1-m) - \beta_m m, \tag{10}$$

$$\frac{dh}{dt} = \alpha_h(1-h) - \beta_h h. \tag{11}$$

Here m, h, and n are mean gate fractions.

For a fixed membrane potential these equations approach steady-state rest values of

$$n(V) \equiv n_\infty(V) = \frac{\alpha_n}{\alpha_n + \beta_n} \tag{12}$$

$$m(V) \equiv m_\infty(V) = \frac{\alpha_m}{\alpha_m + \beta_m} \tag{13}$$

$$h(V) \equiv h_\infty(V) = \frac{\alpha_h}{\alpha_h + \beta_h}. \tag{14}$$

STOCHASTIC THEORY

We want to analyze Eq. 1 with channel kinetics given by the Markov schemes Eqs. 3 and 4 for subthreshold current injection. In particular we wish to examine the generation of spontaneous action potentials due to the fluctuations in the ion channels. Our strategy is to coarse-grain the problem into a continuous time stochastic problem. We will transform the membrane equation into a Langevin equation. The probabilistic nature of the channels will appear as a noise source in the stochastic equation. This will then be analyzed using standard techniques of nonequilibrium statistical mechanics. We will then compare with numerical simulations.

Our analysis depends on the separation of time scales present in the dynamics. We will use approximations that

are similar to those used by Lecar and Nossal (1971a). For a subthreshold injected current the membrane potential is at rest at $V = V_r$. A characteristic time scale can be estimated by linearizing Eq. 1 around the resting potential. Similarly, a characteristic time scale for the currents can be estimated from the kinetic schemes (Eqs. 3 and 4) as well as the deterministic current equations (9–11). The characteristic time scales are given by $\tau_i = (\alpha_i + \beta_i)^{-1}$, where $i = m, h, n$. These time scales are dependent on the parameters used.

For the parameters of Table 1 and zero injected current ($I = 0$), the resting membrane voltage is $V = V_r \sim -65$ mV. At rest, Eq. 1 linearizes to $\dot{V} \sim -0.7V$, implying a time constant of 1.4 ms. The time constants of the m, h, and n currents have the values $\tau_m \sim 0.24$ ms, $\tau_h \sim 8.3$ ms and $\tau_n \sim 5.6$ ms, respectively. For these parameters, the sodium activation current m has a faster time scale than the membrane potential V, which in turn is faster than the currents h and n. An assessment of the time scale separation is given in the Discussion section.

Thus, in the first approximation, the potassium n and the sodium h gate fractions can be considered fixed around their resting values with respect to the membrane potential. It is assumed that the fluctuations of these currents do not play a role in the activation of action potentials. The membrane potential can be considered fixed in the rate constants governing the m current. These assumptions can be checked for self-consistency later. This simplifies the problem greatly. The conductances from Eq. 2 become

$$g_K = \bar{g}_K n_r^4 \tag{15}$$

$$g_{Na} = \bar{g}_{Na} h_r m_3(V, t), \tag{16}$$

where $n_r = n_\infty(V_r)$ and $h_r = h_\infty(V_r)$ (given by Eq. 12 and Eq. 14) and m_3 represents the fraction of open m states. The n and h channel dynamics are "frozen out." This approximation leads to a reduced kinetic scheme for the m current:

$$m_0 \underset{\beta_m}{\overset{3\alpha_m}{\rightleftharpoons}} m_1 \underset{2\beta_m}{\overset{2\alpha_m}{\rightleftharpoons}} m_2 \underset{3\beta_m}{\overset{\alpha_m}{\rightleftharpoons}} m_3. \tag{17}$$

In this approximation the membrane equation (1) is forced by the stationary stochastic variable $m_3(V)$. To characterize the stochastic dynamics of m_3 we require the mean $\langle m_3(V, t)\rangle$ and covariance $\langle \Delta m_3(V, t)\Delta m_3(V, t')\rangle$, where $\Delta m_3(V, t) = m_3(V, t) - \langle m_3\rangle$. The angled brackets represent ensemble averages over the distribution.

The statistical properties of m_3 are readily found for voltage-clamped conditions, where V is fixed. This assumption is based on the separation of time scales between the dynamics of the m variable and the membrane potential. Its validity will be assessed in the Discussion. The kinetic scheme Eq. 17 describes the activity of a channel comprising of three identical gates with opening rate α_m and closing rate β_m. We require the mean and covariance of the fraction or probability of having three open gates for an ensemble of N_{Na} channels. The probability of one m gate being open is given by the steady-state fraction m_∞ given by Eq. 13. The probability for all three gates to be open is m_∞^3, since the gates are independent. Thus the mean of m_3 is given by

$$\langle m_3\rangle = m_\infty^3. \tag{18}$$

For the calculation of the covariance, we first consider a single channel comprised of three identical gates. The covariance of the open state is given by $[\phi(t - t') + m_\infty^2]^3 - m_\infty^6$, where $\phi(t - t') = m_\infty(1 - m_\infty)\exp\{-(\alpha + \beta)|t - t'|\}$ is the covariance of a single gate in the open state (Conti and Wanke, 1975). For an ensemble of N_{Na} channels this yields

$$\langle \Delta m_3(t)\Delta m_3(t')\rangle = [[m_\infty(1 - m_\infty)\exp\{-(\alpha + \beta)|t - t'|\} + m_\infty^2]^3 - m_\infty^6]N_{Na}^{-1}. \tag{19}$$

Setting $t = t'$ in Eq. 19 yields $\langle \Delta m_3^2\rangle = m_\infty^3(1 - m_\infty^3)N_{Na}^{-1}$, which is the expected static variance of a binomial distribution (Lecar and Nossal, 1971b; Tuckwell, 1989). Thus the stochastic variable $m_3(V, t)$ can be represented by $m_3(t) = \langle m_3\rangle + \delta m_3(t)$, where δm_3 is a stochastic variable with zero mean and a variance given by Eq. 19.

From Eq. 19 we find that the decay time of the correlations is less than $(\alpha_m + \beta_m)^{-1}$. This is a much faster time scale than the membrane response time near resting potential. Hence we further approximate the covariance of the stochastic noise by

$$\langle \delta m_3(t)\delta m_3(t')\rangle \simeq 2D(V)N_{Na}^{-1}\delta(t - t'), \tag{20}$$

where

$$2D(V) = N_{Na}\int_{-\infty}^{\infty} \langle \Delta m_3(t)\Delta m_3(0)\rangle \, dt \tag{21}$$

$$= m_\infty^3(1 - m_\infty)\left(\frac{18\alpha_m^2 + 9\alpha_m\beta_m + 2\beta_m^2}{3(\alpha_m + \beta_m)^3}\right). \tag{22}$$

Due to stationarity, the covariance is invariant to a translation in time so t' can be set to zero in the integral without loss of generality. The sodium conductance (16) becomes

$$g_{Na} = \bar{g}_{Na} h_r[m_\infty^3(V) + D^{1/2}(V)N_{Na}^{-1/2}\eta(t)] \tag{23}$$

where $\eta(t)$ is a stochastic variable with statistics

$$\langle \eta(t)\rangle = 0, \quad \langle \eta(t)\eta(t')\rangle = 2\delta(t - t'). \tag{24}$$

It should be noted that the rate constants α_m and β_m remain functions of the membrane potential V.

Substituting Eq. 23 and Eq. 15 into Eq. 1 yields

$$C\frac{dV}{dt} = g(V) + f(V)N_{Na}^{-1/2}\eta(t), \tag{25}$$

where

$$g(V) = -[g_L(V - V_L) + \bar{g}_K n_r^4(V - V_K) + \bar{g}_{Na} h_r m_\infty^3(V)(V - V_{Na})], \tag{26}$$

$$f(V) = -\bar{g}_{Na}h_r(V - V_{Na})D^{1/2}(V). \quad (27)$$

Equation 25 is a one-dimensional Langevin equation driven by a voltage-dependent thermal white noise. The function $g(V)$ can be considered to be the negative gradient of a potential function $v(V)$, i.e., $g(V) = -v'(V)$. Equation 25 is directly analogous to the motion of an overdamped particle (friction dominated) moving within a potential well $v(V)$ and driven by thermal fluctuations. The membrane potential V corresponds to the location of the particle, the capacitance C plays the role of a friction coefficient, and the inverse number of channels N_{Na}^{-1} plays the role of temperature. In this analogy, the velocity of the particle is balanced by the forces acting on it. The inertial effects are ignored. The potential function $v(V)$ has the shape of a double well. One minimum is at the resting voltage V_r. In order for an action potential to be generated the particle (membrane potential) must surmount the barrier and cross to the other minimum. In the purely deterministic equation this is achieved when the injected current exceeds a threshold level. In terms of the double well analogy the constant injected current corresponds to a "tilt" of the potential well. At threshold the tilt is sufficient to negate the local minimum near the resting potential. The particle is then free to "roll" to the other minimum. The other degrees of freedom, frozen in this particular analysis, bring the particle back to rest.

With the addition of channel noise, action potentials can be generated spontaneously for a subthreshold injected current. The thermal noise can occasionally "kick" the membrane potential over the barrier. Once over the barrier, an action potential results and the slow degrees of freedom will bring the potential back to resting level. The mean firing rate can then be approximated by the mean escape rate of the membrane potential over the barrier. The rate for a particle to escape over a potential barrier due to thermal noise is a classic problem addressed by Kramers (1940). Kramers' calculation of the escape rate relies on an assumption of approximate stationarity which requires a relatively low temperature compared to the barrier height. Thus our analysis will become less accurate as the number of channels decreases (temperature increases). In addition, this analysis ignores the refractory time and dynamics to restore the potential back to rest. This will be a small effect if the escape time is slower than the refractory time.

There is an added difficulty in the analysis of Eq. 25 because the noise amplitude is a function of the membrane potential. This is referred to as a multiplicative noise process. However, this system can be transformed to a system with additive noise by dividing through by $f(V)$ and using the transformation $dV/dy = f(V)$ or

$$y = \int^{V} \frac{dV'}{f(V')} \equiv w(V), \quad (28)$$

to yield

$$C\frac{dy}{dt} = H(y) + N^{-1/2}\eta(t), \quad (29)$$

where

$$H(y) = \frac{g(w^{-1}(y))}{f(w^{-1}(y))} \equiv -U'(y). \quad (30)$$

Here $U(y)$ is an effective potential for the dynamics given by Eq. 29.

In the region of interest, $f(V)$ is monotonic so the double well shape is preserved in the effective potential well $U(y)$. The resulting equation is now the classic barrier escape problem with simple additive thermal noise. Kramers' formula for the escape rate applied to Eq. 29 is given by (Kramers, 1940; Risken, 1989)

$$R_K \sim \frac{1}{2\pi}\sqrt{U''(y_{min})|U''(y_{max})|} \times \exp\left(-C[U(y_{max}) - U(y_{min})]N_{Na}\right), \quad (31)$$

where y_{min} is the position of the resting minimum, and y_{max} is the position of the barrier maximum. A simple derivation of this formula is given by Risken (1989). Note the negative exponential dependence on the number of sodium channels N_{Na}.

The numerical quantities in R_K can be computed without actually inverting the integral relation (Eq. 28). In Eq. 31, y_{min} and y_{max} are two of the roots of the equation

$$H(y) = \frac{g(w^{-1}(y))}{f(w^{-1}(y))} = 0. \quad (32)$$

Because $f(V)$ is well-behaved, these roots are given by

$$y_{min} = w(V_{min}), \quad y_{max} = w(V_{max}), \quad (33)$$

where $V = V_{min} \equiv V_r$ and $V = V_{max}$ are the two corresponding roots of $g(V)$. These roots can be solved for numerically. All quantities in Eq. 31 can be evaluated using V_{min} and V_{max}. In particular

$$U(y_{max}) - U(y_{min}) = \int_{y_{min}}^{y_{max}} U'(y)\,dy = -\int_{V_{min}}^{V_{max}} \frac{g(V)}{f(V)}\frac{dy}{dV}dV = -\int_{V_{min}}^{V_{max}} \frac{g(V)}{f^2(V)}dV. \quad (34)$$

and

$$U''(y)|_{y=y_0} = \frac{d}{dy}\left(\frac{g(y)}{f(y)}\right)\bigg|_{y_0} = \left[\frac{d}{dV}\left(\frac{g(V)}{f(V)}\right)f(V)\right]_{V_0} = g'(V_0), \quad (35)$$

using the fact that $h(V_0) = 0$ for $V_0 = V_{min}, V_{max}$. Using Eqs. 34 and 35 in Eq. 31 renders the expression for the firing rate in closed form.

Using the parameters given in Table 1 and solving $g(V) = 0$ numerically yields three roots at $V_{min} \equiv V_r = -65.0$ mV, $V_{max} = -62.4$ mV, and $V_3 = 48.9$ mV, where V_3 is the location of the other minimum. Thus a spontaneous action potential is generated if the channel noise can "kick" the membrane voltage beyond the barrier peak at $V = V_{max} = -62.4$ mV. The voltage range between V_r and V_{max} is relatively small. In this region, the channel rates remain close to their resting values so the approximations used are self-consistent. Once over the barrier the membrane potential continues increasing until it reaches $V \sim V_3$ whereupon the h and n channels become dominant and restore V to rest.

The integral in equation (34) can be evaluated numerically with the result $U(y_{max}) - U(y_{min}) = 0.000225$. Using Eq. 35 we find that $U''(y_{min}) = 0.246$ and $U''(y_{max}) = -0.321$. Substituting these values into Eq. 31 yields

$$R_K \sim 45 \exp[-N_{Na}/4440]s^{-1}. \quad (36)$$

Using the sodium density in Table 1 this can be reexpressed as

$$R_K \sim 45 \exp[-\text{Area}/(74\mu m^2)]s^{-1}. \quad (37)$$

The probability density function (PDF) for the interspike intervals can also be estimated. The firing of action potentials is governed by a barrier escape process which has statistics similar to a simple Poisson process (Risken, 1989). This implies a negative exponential PDF for the interspike intervals. This is not entirely the case because there is a refractory time, or "dead time," immediately after an action potential. The distribution of interspike intervals is better described by a modified dead-time Poisson process with a PDF for the interspike intervals τ approximately given by

$$P(\tau) \simeq R_K(N_{Na}) \exp[-R_K(N_{Na})(\tau_0 - \tau_R)]\Theta(\tau - \tau_R), \quad (38)$$

where $\Theta(s)$ is the unit step function, τ_R is the average refractory time. In actuality the refractory time will itself also be a stochastic variable due to the discrete channel effects. The PDF for the interspike intervals will then be a convolution of Eq. 38 with the PDF governing the refractory time. The result will be similar to Eq. 38, but the step function will be "smoothed" out.

These theoretical results are compared to numerical simulations of the full stochastic system in the next section. It should be noted that the calculation could be easily adapted to a variety of excitable membrane equations. The essential ingredient is that there be a separation of time scales. The crucial approximation was that only the activation gate of the Na^+ channel was important for action potential generation. These assumptions should hold for a large class of neuronal models.

NUMERICAL SIMULATIONS

For comparative purposes, we simulated the complete system of discrete ion channels given by the kinetic diagrams of Eqs. 3 and 4. Problems of this type can be solved using a variety of methods (Skaugen and Walløe, 1979). Conceptually, the simplest such algorithm would simply keep track of the states of N_{Na} sodium channels and N_K potassium channels. For each channel in state x at time t_0, the probability of remaining in that state for more than t seconds is given by the relationship $\exp[-\gamma_x t]$, where γ_x is the sum of all rate constants associated with escape from state x. (For example, for a potassium channel in state $x = n_3$, $\gamma_x = \alpha_n + 3\beta_n$; see Eqs. 3 and 4.) From this relationship, it follows that the probability density function associated with the lifetime of a single channel in state x is $f(t) = \gamma_x \exp[-\gamma_x t]$. To pick a transition time t_{tr} from this PDF, one can draw a pseudorandom number r_1 from the uniform distribution [0, 1] and apply the transformation $t_{tr} = \ln(r_1^{-1})/\gamma_x$. An algorithm of this architecture would pick transition times for each channel in the system, then, using the smallest picked transition time, update the membrane potential, update the state of the correct channel, and start anew.

Although an algorithm like that above is conceptually appealing, it is difficult to implement and grossly inefficient. A far better algorithm takes advantage of the statistical independence and memorylessness of parallel ion channels. In this formulation, which follows previous work by Gillespie (1977) and Skaugen and Walløe (1979), the states of individual ion channels are not tracked, but rather the number of ion channels in each of the 13 states of Eqs. 3 and 4 is followed. The lifetime in a particular state ($N_{n_0} = x_1$, $N_{n_1} = x_2$, . . . , $N_{m_3h_0} = x_{13}$) at $t = t_0$ has the PDF

$$f(t) = \lambda \exp[-\lambda(t - t_0)], \quad t \geq t_0 \quad (39)$$

where

$$\lambda = \sum_{i=0}^{3} \sum_{j=0}^{1} N_{m_ih_j}\gamma_{ij} + \sum_{k=0}^{4} N_{n_k}\zeta_k \quad (40)$$

In Eq. 40, $N_{m_ih_j}$ is the number of sodium channels in state m_ih_j, N_{n_k} is the number of potassium channels in state n_k, γ_{ij} is the sum of rate constants associated with escapes from state m_ih_j, and ζ_k is the sum of rate constants associated with escapes from state n_k. (For example, $\gamma_{10} = \beta_m + \alpha_h + 2\alpha_m$; see Eqs. 3 and 4.) Equation 40 accounts for the 13 state variables and 28 state transitions of the Markov kinetic scheme for the Hodgkin-Huxley model.

The transition time t_{tr} from the current state into its immediate successor is determined by drawing a pseudorandom number r_1 from the uniform distribution [0, 1] and using the transformation $t_{tr} = \ln(r_1^{-1})/\lambda$. Once t_{tr} is determined, the membrane potential is updated to the new current time $t = t_0 + t_{tr}$ by integrating Eq. 1.

The next step in the stochastic algorithm is to determine which of 28 possible state transitions occurred at t_{tr}. The conditional probability that state transition j occurred in the infinitesimally small time slice $[t_{tr}, t_{tr} + dt]$ is given by the ratio

$$\frac{a_j dt}{\sum_{i=0}^{27} a_i dt} = \frac{a_j}{\sum_{i=0}^{27} a_i} \quad (41)$$

where a_j ($0 \leq j \leq 27$) is the product of the rate constant associated with transition j and the number of channels currently in the parent state associated with that transition. For example, if transition 1 represents the transition of a potassium channel from having 0 open n gates to having 1 open n gate, $a_1 = 4\alpha_n N_{n_0}$. Because the sum in the denominator of Eq. 41 is simply a reordered version of Eq. 40, Eq. 41 also equals a_j/λ. In the algorithm, the specific transition that occurred at time t_{tr} is determined by drawing a random variable ν from the uniform distribution [0, λ], and determining μ such that

$$\sum_{i=0}^{\mu-1} a_i < \nu \leq \sum_{i=0}^{\mu} a_i \qquad (42)$$

The value of μ, which represents the transition that occurred, is used to update the count of channels in each state. Next, values of all voltage-dependent rate constants are updated and the process is continued by finding the next transition time.

This algorithm has two principal advantages over an algorithm that tracks individual ion channels. First, because the total number of channels in a given state is tracked, the present algorithm requires less bookkeeping. Second, and most importantly, the current algorithm requires the generation of only two random numbers per time step, compared with $N_{Na} + N_K$ for the more traditional algorithm. This enormous reduction in required pseudorandom numbers leads to much faster execution and less stringent requirements on the random number generator.

The present stochastic algorithm relies on two assumptions that could potentially lead to errors. First, it is dependent on a high-quality algorithm for generating pseudorandom, uniformly distributed numbers. For these studies, the algorithm of Press and colleagues (1992) was used. Second, it is assumed that the rate constants of Eqs. 3 and 4 do not change significantly during a single time step. Because transitions occur very frequently in practice, errors due to violation of this assumption are small.

The accuracy of the algorithm was checked three ways. First, simulation results were compared with those of Skaugen and Walløe (1979) and found to agree. Second, both spontaneous and driven results with large areas were compared with results from the deterministic Hodgkin-Huxley model, generated using the simulation package NEURON (Hines, 1989). Third, simulation results under both current and voltage clamp conditions were compared with analytically derived results in the previous section.

A set of simulations was performed in which the membrane potential was held constant at −65 mV. In these simulations, $N_{m_3h_1}$, the number of open Na^+ channels of a total of $N_{Na} = 6000$, was tracked at intervals of 0.01 ms. The autocorrelation function generated from these records is shown in Fig. 1 (*closed symbols*). Also shown is the predicted relationship from the stochastic theory (*solid line*) obtained by multiplying Eq. 19 by $h_r N_{Na}^2$. The predicted and measured traces are in excellent agreement, particularly for times <0.5 ms. For greater times, there is slightly more divergence, perhaps because of the effects of the slower inactivation process, considered "frozen" in Eq. 19.

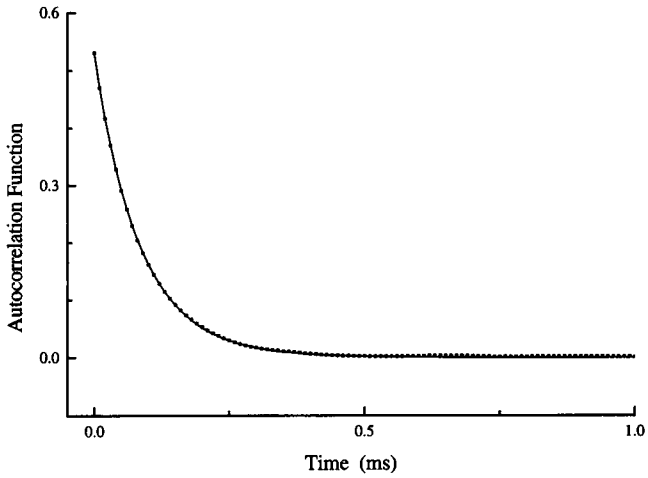

FIGURE 1 Predicted and modeled autocorrelation functions. Symbols show the numerically calculated autocorrelation function of the number of open Na^+ channels ($N_{m_3}h_1$) for a simulation of a 10-s epoch under voltage clamp at a potential of −65 mV for a membrane patch of 100 μm^2. The sampling interval was 0.01 ms. The solid line shows the theoretically predicted autocorrelation function, obtained by multiplying Eq. 19 by $h_r N_{Na}^2$.

Figure 2 shows output from the simulations under current clamp, with $I = 0$, for six values of membrane area. As has

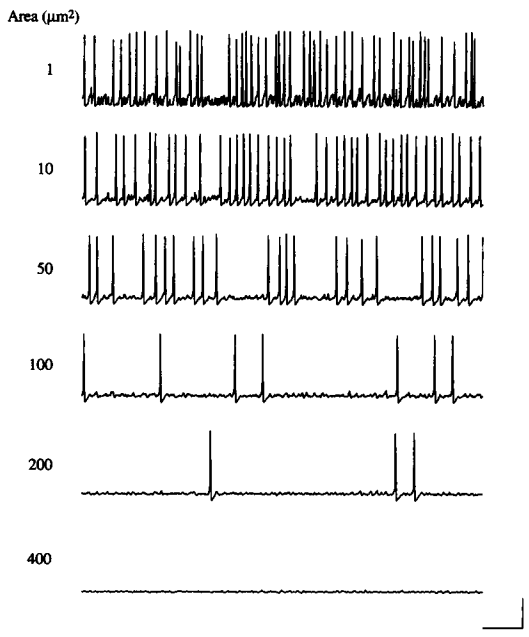

FIGURE 2 Spontaneous output from the simulations under current clamp. Applied current is zero in all cases. To the left of each trace is the area of the membrane, which was used, along with channel densities from Table 1, to calculate N_{Na} and N_K. Vertical scale: 50 mV. Horizontal scale: 100 ms.

been noted previously, the spontaneous rate is high for small membrane areas, which correspond to small numbers of channels. As the membrane area is increased, the rate of spontaneous action potentials approaches zero, the expected rate from the deterministic model.

Average rate results from several runs are shown in Fig. 3, along with the predicted relationship from Eq. 37. Simulated and predicted results agree well except at very small values of area. For these values, openings of a small number of channels can generate anomalous spikes not accounted for by the present theory. A least-squares fit of a decaying exponential function to the last four points from the numerical results gives a magnitude of 42 Hz and a decay constant of 71 μm^2. (Compare theoretical values of 45 Hz and 74 μm^2.)

Simulation results were examined in terms of interspike interval distributions as well. Figure 4 shows an ISI histogram, generated from three 10-s runs with $Area = 100\ \mu m^2$. Values have been normalized to have unit area (i.e., each value has been divided by bin width and the total number of intervals in the ISI set.) The trace is the predicted relationship from Eq. 38, with R_K calculated from Eq. 37 and a constant refractory period of 18 ms, picked as the minimum interspike interval seen in the simulated data. Again, agreement between predicted and simulated results is good. Together, Figures 3 and 4 indicate that both the average rate of firing and the PDF of interspike intervals are determined largely by the Na^+ activation process alone. Thus, these results support the major assumption of our analytic analysis.

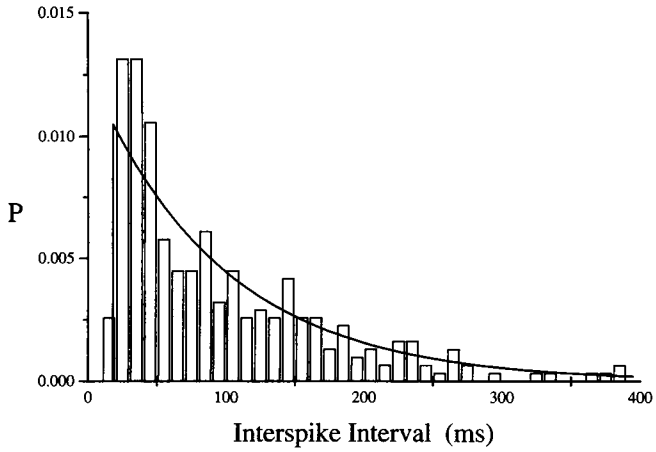

FIGURE 4 Interspike intervals from simulations agree with the predicted PDF. Open bars show the interspike interval histogram for spontaneous action potentials with surface area = 100 μm^2. Values have been divided by bin width and total number of spikes. The solid trace shows the predicted PDF for the system under these conditions, calculated from Eq. 38 with a refractory period of 18 ms and average rate of 10.5 spikes/s.

DISCUSSION

We have analyzed the spontaneous firing rate for the Hodgkin-Huxley system with random channel kinetics. We focused on finding closed-form expressions for the firing rate as a function of the number of ion channels and the probability density function for the interspike intervals. We then performed accurate numerical simulations of the full stochastic system to test our analytical predictions. The theoretical results match the numerical results very well, as seen in Figure 3. Given that the firing rate is related to the first passage time of a stochastic problem, the probability density function for the interspike intervals can also be estimated. For a purely Poisson process this will be given by a negative exponential. However, in the case of the excitable membrane, there is a refractory time which can be accounted for by shifting the negative exponential. As seen in Figure 4, this approximation is fairly good. It captures the mean and variance of the distribution.

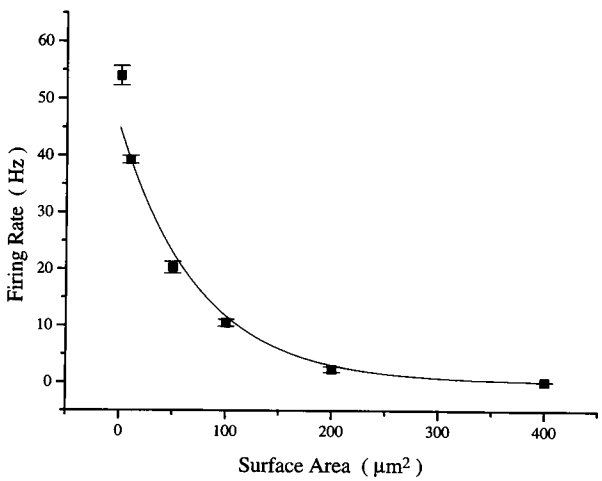

FIGURE 3 Spontaneous rate of the model as a function of membrane surface area. Symbols are mean (± standard deviation) values of spontaneous firing rate, generated from three runs of 10 s (model time) each. The solid line shows the predicted mean firing rate, calculated from Eq. 37. Predicted and observed firing rates are in good agreement for all but the smallest values of surface area.

Our analytical approach was to reduce the problem of action potential generation to a simple barrier escape problem. The firing rate was approximated by the mean first passage time or barrier escape time. This was accomplished by a series of approximations that relied on the separation of time scales inherent in the problem. For the classic squid giant axon parameters used, the calculation was highly successful. Our approximations should hold even when the separation of time scales is not exceedingly large. The calculation required that the h and n currents could be considered fixed at their resting values. Near resting potential, the effect of the n current is very small, and thus approximation errors are not important. The deactivating current h has a significant value near rest and does play an important role. The multiplicative nature of the noise diminishes its influence. Both the potential well and the noisy forcing have the same factor of h in the Langevin equation 25. Thus, the effect of h is "scaled" away. This is best seen

in the transformation to the Langevin equation with additive noise 29. Also essential to the calculation was that the membrane potential be considered fixed (voltage-clamped) when calculating the statistical properties of the stochastic variable m_3. This approximation requires a wide separation of time scales between the membrane potential and the fast activating m current. The multiplicative noise again plays a role. The noise amplitude is very small below resting potential and increases sharply beyond threshold at $V = V_{max}$. This changes the effective shape of the well, creating a very sharp dropoff beyond threshold. Once the membrane potential reaches threshold, action potential generation ensues quickly. Thus, only the dynamics between rest and threshold need to be captured. The distance between rest and threshold is small (2.6 mV) so over this interval, the reaction rates (α_m and β_m), and the asymptotic fraction m_∞, do not vary much. The crucial time scale here may be the response time of m_3 compared to the dwell time in the well (firing time). The firing time is on the order of 20 ms and the response time is around 0.24 ms, which is a wide separation.

We do not have a definite criterion for the applicability of our method. However, we are confident that our results will be very accurate for any parameter set with fairly modest time scale separations such as those used in this paper. Our analytical method is not limited to the Hodgkin-Huxley system. It could easily be generalized to any excitable membrane equation which has a fast activating current and slow recovery currents compared to the membrane time scale near rest. For the Hodgkin-Huxley system, the roots of a transcendental equation were required and were solved for numerically. However, for simple polynomial equations such as the Fitzhugh-Nagumo equation, a completely analytical result could be obtained.

Our formalism could be applied to understanding the effect of channel noise on suprathreshold firing. In this case the firing rate would not be given by a barrier escape time. In the suprathreshold regime the deterministic dynamics will bring the membrane potential to threshold. However, the channel noise will cause this path to fluctuate. The firing time can be estimated by evaluating the mean first passage time from rest to threshold of this stochastic process. Our reduced description could also possibly be useful for understanding the propagation of action potentials. The one-dimensional Langevin equation could be generalized to a spatially extended "cable" equation. However, this would be only useful in understanding the propagation of an "action potential front," because the restoration dynamics are not included.

Experimental verification of our results could involve comparing recordings made at the cellular level with those made using membrane patches of different sizes. Interpretation of these experiments would be difficult unless one could demonstrate that Na^+, K^+, and leak channels are distributed evenly on the cell membrane. Another approach, that of blocking different fractions of the Na^+ channels with low concentrations of tetrodotoxin, would be greatly complicated by the need to keep the ratio of Na^+, K^+, and leak channels constant.

The effects of ion channel fluctuations may be macroscopically relevant. For example, it has been argued that such fluctuations in muscarinic K^+ channels may contribute to the heart rhythm in the sino-atrial node (Ito et al., 1994). In neuronal structures with relatively small surface areas, such as nodes of Ranvier, the macroscopic effects of ion channel noise seem to be important in determining observed distributions in the threshold for generation of action potentials (Lecar and Nossal, 1971a; Rubinstein, 1995; Sigworth, 1980). Our results indicate that channel fluctuations may account for spontaneous activity in these structures as well. We predict a characteristic displaced negative exponential distribution of interspike intervals that is often seen experimentally. For the Markov representation of the Hodgkin-Huxley model, the mean firing rate and interspike interval distribution need not be calculated via time-consuming simulations, but rather can be estimated analytically using Eqs. 36 and 38. It is our hope that the presence of such simplified methods will spur more activity in this area.

We would like to thank John Rinzel for originally suggesting this problem and Haim Sompolinsky for stimulating discussions.

This work was started at the Marine Biological Laboratory, in the Methods in Computational Neuroscience course, directed by David Tank and David Kleinfeld. This work was supported by the National Science Foundation (C.C.) and the Whitaker Foundation (J.W.).

REFERENCES

Chandler, D. 1987. Introduction to modern statistical mechanics. Oxford University Press, New York.

Conti, F., and E. Wanke. 1975. Channel noise in nerve membranes and lipid bilayers. *Q. Rev. Biophys.* 8:451–506.

De Felice, L. J., and W. N. Goolsby. 1996. Order from randomness: spontaneous firing from stochastic properties of ion channels. In Fluctuations and Order: The New Synthesis. M. Millonas, editor. Springer, New York. 331–342.

Fox, R. F., and Y. Lu. 1994. Emergent collective behavior in large numbers of globally coupled independently stochastic ion channels. *Physical Review E* 49:3421–3431.

Gillespie, D. T. 1977. Exact stochastic simulation of coupled chemical reactions. *J. Phys. Chem.* 81:2340–2361.

Hille, B. 1992. Ionic Channels of Excitable Membranes, 2nd ed. Sinauer Associates, Sunderland, MA.

Hines, M. 1989. A program for simulation of nerve equations with branching geometries. *Int. J. Biomed. Comput.* 24:25–68.

Hodgkin, A. L., and A. F. Huxley. 1952. A quantitative description of membrane current and its application to conduction and excitation in nerve. *J. Physiol.* 10:500–544.

Ito, H., K. Ono, and A. Noma. 1994. Background conductance attributable to spontaneous opening of muscarinic K^+ channels in rabbit sino-atrial node. *J. Physiol.* 476:55–68.

Kramers, H. A. 1940. Brownian motion in a field of force and the diffusion model of chemical reactions. *Physica* 7:284.

Lecar, H., and R. Nossal. 1971a. Theory of threshold fluctuations in nerves. I. Relationships between electrical noise and fluctuations in axon firing. *Biophys. J.* 11:1048–1067.

Lecar, H., and R. Nossal. 1971b. Theory of threshold fluctuations in nerves. I. Analysis of various sources of membrane noise. *Biophys. J.* 11:1068–1084.

Press, W. H., S. A. Teukolsky, W. T. Vetterling, and B. P. Flannery. 1992. Numerical Recipes. 2nd ed. Cambridge University Press, Cambridge, U.K.

Risken, H. 1989. The Fokker-Planck Equation. 2nd ed. Springer-Verlag, Berlin.

Rubinstein, J. T. 1995. Threshold fluctuations in an N sodium channel model of the node of Ranvier. *Biophys. J.* 68:779–785.

Sigworth, F. J. 1980. The variance of sodium current fluctuations at the node of Ranvier. *J. Physiol.* 307:97–129.

Skaugen, E., and L. Walløe. 1979. Firing behaviour in a stochastic nerve membrane model based upon the Hodgkin-Huxley equations. *L. Acta Physiol. Scand.* 107:343–363.

Strassberg, A., and L. J. De Felice. 1993. Limitations of the Hodgkin-Huxley formalism: effects of single channel kinetics on transmembrane voltage dynamics. *Neural Computation.* 5:843–855.

Tuckwell, H. C. 1989. Stochastic Processes in the Neurosciences. SIAM, Philadelphia.